

Stiff equation-of-state of neutron star due to antikaon condensation

K. Miyazaki

E-mail: miyazakiro@rio.odn.ne.jp

Abstract

We re-examine the antikaon condensation in neutron star (NS) matter within the extended Zimanyi-Moszkowski model. The meson-kaon coupling constants are independent of mean-field and are determined to reproduce kaon potential $U_{\bar{K}}(\rho_{NM}) = -120\text{MeV}$, -140MeV or -170MeV in a saturated nuclear matter. In contrast to all the preceding works, we find that a deeper kaon potential produces a stiffer EOS. This is because the abundance of antikaons tends to exclude Ξ s in NS matter and so the strange scalar mean-field becomes weaker. For $U_{\bar{K}}(\rho_{NM}) = -120\text{MeV}$ there are no antikaons in NSs, and the massive NSs of $M_G > 1.6M_\odot$ are not reproduced although we have found a branch for the third family of compact stars. The result for $U_{\bar{K}}(\rho_{NM}) = -140\text{MeV}$ reproduces the massive NSs but not the mass and radius of EXO 0748-676. Only the result using the very deep kaon potential $U_{\bar{K}}(\rho_{NM}) = -170\text{MeV}$ is satisfactory. This is consistent to the recent experimental information on K^- atom and deeply bound kaonic states. Consequently, the antikaon condensed phase is likely to exist in NSs.

1 Introduction

Owing to the recent vigorous observations and discoveries, the neutron stars (NSs) have been providing valuable information on an equation-of-state (EOS) [1] of dense nuclear matter. Now, the discovered massive NSs [2-9] and the observed large radii [10-12] strongly suggest a stiff EOS. They are reproduced by the relativistic mean-field (RMF) models of NS matter that assume the density-dependent [13] or the field-dependent [14] meson-nucleon coupling constants. However, if we take into account hyperons together with nucleons [15,16], the EOS becomes much softer and so cannot reproduce the massive NSs. The soft EOSs due to hyperons are common to the other models [17-21] of NS matter. In the case of the extended Zimanyi-Moszkowski (EZM) model, the gravitational mass of the most massive NS is $M_G = 2.17M_\odot$ [14] if only nucleons are considered as baryons, while it decreases to $M_G = 1.57M_\odot$ [16] if all the baryon octets are considered. Although there is a little information on nucleon-hyperon (NY) and hyperon-hyperon (YY) interactions, the meson-hyperons coupling constants in Ref. [16] are the most reasonable ones at present. To the contrary, the artificial adjustment of the coupling

constants as in Ref. [22] is physically meaningless. We are therefore confronted a serious difficulty.

So as to resolve the problem, we have to improve the model itself or consider the other constituents than baryons. In the present work we extend the EZM model in Ref. [16] so as to take into account the antikaon condensation in NS matter. Some colleagues will object to the idea because the antikaons do not directly contribute to the pressure of hadronic matter and so in all the preceding investigations [23-25] the additional inclusion of antikaons to hyperons softens the EOSs further. In fact, we formerly investigated [26] the antikaon condensation in the EZM model and obtained a rather soft EOS. Moreover, in a subsequent paper [27] that considered the field-dependent meson-kaon coupling constants, the maximum mass of NS was lower than the canonical value $M_G = 1.44M_\odot$ [28] so that the antikaon condensation was unlikely in NS matter. However, we re-investigate the antikaon condensation using the different formulation and calculus from Ref. [27], which are presented in the next section. We will find in section 3 that the antikaon condensation stiffens the EOS because of its effect to exclude hyperons in NS matter.

2 Antikaons in the EZM model

The EZM model Lagrangian of NS matter composed of baryon octets and leptons is the same as Ref. [16]. The corresponding energy density is

$$\begin{aligned} \mathcal{E}_F = & \frac{1}{4} \sum_{\substack{B=p,n,\Lambda,\Sigma^+, \\ \Sigma^0,\Sigma^-, \Xi^0,\Xi^-}} (3E_{FB}^* \rho_B + M_B^* \rho_{SB}) + \sum_B V_B \rho_B + \frac{1}{4} \sum_{l=e^-, \mu^-} (3E_{Fl} \rho_l + m_l \rho_{Sl}) \\ & + \frac{1}{2} m_\sigma^2 \langle \sigma \rangle^2 + \frac{1}{2} m_\delta^2 \langle \delta_3 \rangle^2 + \frac{1}{2} m_{\sigma^*}^2 \langle \sigma^* \rangle^2 - \frac{1}{2} m_\omega^2 \langle \omega_0 \rangle^2 - \frac{1}{2} m_\rho^2 \langle \rho_{03} \rangle^2 - \frac{1}{2} m_\phi^2 \langle \phi_0 \rangle^2, \end{aligned} \quad (1)$$

where ρ_B and ρ_l are the vector densities of baryons and leptons in NS matter, ρ_{SB} and ρ_{Sl} are their scalar densities, and E_{FB}^* and E_{Fl} are their Fermi energies. The m_σ *etc.* are masses of the mesons and $\langle \sigma \rangle$ *etc.* are their mean-fields. The effective mass M_B^* of each baryon is

$$M_B^* = m_B^* M_B = M_B + S_B. \quad (2)$$

The scalar potential S_B is given by

$$S_B = -g_{BB\sigma}^* \langle \sigma \rangle - g_{BB\delta}^* \langle \delta_3 \rangle I_{3B} - g_{BB\sigma^*}^* \langle \sigma^* \rangle, \quad (3)$$

where $I_{3B} = \{1, -1, 0, 1, 0, -1, 1, -1\}$ for $B = \{p, n, \Lambda, \Sigma^+, \Sigma^0, \Sigma^-, \Xi^0, \Xi^-\}$ and $g_{BB\sigma}^*$ *etc.* are the renormalized field-dependent scalar-meson coupling constants [16]. On the

other hand, the vector potential V_B is given by

$$V_B = g_{BB\omega}^* \langle \omega_0 \rangle + g_{BB\rho}^* \langle \rho_{03} \rangle I_{3B} + g_{BB\phi}^* \langle \phi_0 \rangle, \quad (4)$$

where $g_{BB\omega}^*$ *etc.* are the renormalized vector-meson coupling constants [16].

Next, we have to add the contribution of antikaons to Eq. (1). In the present work we assume the same form of the energy density as Ref. [29]:

$$\mathcal{E}_K = \frac{1}{2} \sum_{\bar{K}=\bar{K}^0, K^-} (f \theta_{\bar{K}})^2 (\alpha_{\bar{K}} + \mu_{\bar{K}}^2), \quad (5)$$

where f is the pion decay constant, $\theta_{\bar{K}}$ is the condensate amplitude. The antikaon chemical potentials are

$$\mu_{\bar{K}^0} = 0, \quad (6)$$

$$\mu_{K^-} = \mu_{e^-}, \quad (7)$$

where μ_{e^-} is an electro-chemical potential in β -equilibrated NS matter.

There are two definitions [23,30] of the effective kaon mass $M_{\bar{K}}^*$ in dense hadronic matter. We here assume the definition in Ref. [30]:

$$M_{\bar{K}}^* = M_K - g_{KK\sigma} \langle \sigma \rangle - g_{KK\delta} I_{3\bar{K}} \langle \delta_3 \rangle - g_{KK\sigma^*} \langle \sigma^* \rangle, \quad (8)$$

where $M_K = 495.7\text{MeV}$ is the free kaon mass and $I_{3\bar{K}} = \{1, -1\}$ for $\bar{K} = \{\bar{K}^0, K^-\}$. Then, $\alpha_{\bar{K}}$ in Eq. (5) is given by [29]

$$\alpha_{\bar{K}} = M_{\bar{K}}^{*2} - V_{\bar{K}}^2, \quad (9)$$

where the kaon vector potential is

$$V_{\bar{K}} = -g_{KK\omega} \langle \omega_0 \rangle + g_{KK\rho} \langle \rho_{03} \rangle I_{3\bar{K}} - g_{KK\phi} \langle \phi_0 \rangle. \quad (10)$$

The essential difference of the present work from Ref. [27] is to use the free meson-kaon coupling constants $g_{KK\sigma}$ *etc.* in Eqs. (8) and (10) rather than the renormalized ones in Eqs. (9) and (10) of Ref. [27].

Because the three scalar mean-fields $\langle \sigma \rangle$, $\langle \delta_3 \rangle$ and $\langle \sigma^* \rangle$ are expressed in terms of the three independent effective masses m_p^* , m_n^* and m_Λ^* , the effective masses of the other baryons and antikaons are also expressed by them. Similarly, because the three vector mean-fields $\langle \omega_0 \rangle$, $\langle \rho_{03} \rangle$ and $\langle \phi_0 \rangle$ are expressed in terms of the three independent vector potentials V_p , V_n and V_Λ , the vector potentials of the other baryons and antikaons are also expressed by them. The renormalized meson-baryon coupling constants are also functions of the effective masses. Then, m_p^* , m_n^* and m_Λ^* , and V_p , V_n and V_Λ are determined from

extremizing the energy density $\mathcal{E}_F + \mathcal{E}_K$ by them:

$$\begin{aligned}
 & C_{VN}\rho_p + \sum_{Y \neq \Lambda} \left(g_{nn\rho}^* g_{YY\omega}^* + g_{nn\omega}^* g_{YY\rho}^* I_{3Y} - C_{V\Lambda} g_{nn\rho}^* g_{YY\phi}^* \right) \rho_Y \\
 & + \sum_{\bar{K}} \left(g_{nn\rho}^* g_{KK\omega} - g_{nn\omega}^* g_{KK\rho} I_{3\bar{K}} - C_{V\Lambda} g_{nn\rho}^* g_{KK\phi} \right) V_{\bar{K}} (f \theta_{\bar{K}})^2 \\
 & - m_\omega^2 g_{nn\rho}^* \langle \omega_0 \rangle - m_\rho^2 g_{nn\omega}^* \langle \rho_{03} \rangle + C_{V\Lambda} m_\phi^2 g_{nn\rho}^* \langle \phi_0 \rangle = 0,
 \end{aligned} \tag{11}$$

$$\begin{aligned}
 & C_{VN}\rho_n + \sum_{Y \neq \Lambda} \left(g_{pp\rho}^* g_{YY\omega} - g_{pp\omega}^* g_{YY\rho} I_{3Y} - C_{V\Lambda} g_{pp\rho}^* g_{YY\phi}^* \right) \rho_Y \\
 & + \sum_{\bar{K}} \left(g_{pp\rho}^* g_{KK\omega} + g_{pp\omega}^* g_{KK\rho} I_{3\bar{K}} - C_{V\Lambda} g_{pp\rho}^* g_{KK\phi} \right) V_{\bar{K}} (f \theta_{\bar{K}})^2 \\
 & - m_\omega^2 g_{pp\rho}^* \langle \omega_0 \rangle + m_\rho^2 g_{pp\omega}^* \langle \rho_{03} \rangle + C_{V\Lambda} m_\phi^2 g_{pp\rho}^* \langle \phi_0 \rangle = 0,
 \end{aligned} \tag{12}$$

$$\sum_Y g_{YY\phi}^* \rho_Y + \sum_{\bar{K}} g_{KK\phi} V_{\bar{K}} (f \theta_{\bar{K}})^2 - m_\phi^2 \langle \phi_0 \rangle = 0, \tag{13}$$

$$\begin{aligned}
 & M_N \rho_{Sp} + \sum_{Y \neq \Lambda} \frac{\partial m_Y^*}{\partial m_p^*} M_Y \rho_{SY} + M_N \sum_{Y \neq \Lambda} \frac{\partial V_{0Y}}{\partial M_p^*} \rho_Y \\
 & + M_N \sum_{\bar{K}} (f \theta_{\bar{K}})^2 \left(M_{\bar{K}}^* \frac{\partial M_{\bar{K}}^*}{\partial M_p^*} - V_{\bar{K}} \frac{\partial V_{\bar{K}}}{\partial M_p^*} \right) \\
 & + m_\sigma^2 \langle \sigma \rangle \frac{\partial \langle \sigma \rangle}{\partial m_p^*} + m_\delta^2 \langle \delta_3 \rangle \frac{\partial \langle \delta_3 \rangle}{\partial m_p^*} + m_{\sigma^*}^2 \langle \sigma^* \rangle \frac{\partial \langle \sigma^* \rangle}{\partial m_p^*} \\
 & - m_\omega^2 \langle \omega_0 \rangle \frac{\partial \langle \omega_0 \rangle}{\partial m_p^*} - m_\rho^2 \langle \rho_{03} \rangle \frac{\partial \langle \rho_{03} \rangle}{\partial m_p^*} - m_\phi^2 \langle \phi_0 \rangle \frac{\partial \langle \phi_0 \rangle}{\partial m_p^*} = 0,
 \end{aligned} \tag{14}$$

$$\begin{aligned}
 & M_N \rho_{Sn} + \sum_{Y \neq \Lambda} \frac{\partial m_Y^*}{\partial m_n^*} M_Y \rho_{SY} + M_N \sum_{Y \neq \Lambda} \frac{\partial V_{0Y}}{\partial M_n^*} \rho_Y \\
 & + M_N \sum_{\bar{K}} (f \theta_{\bar{K}})^2 \left(M_{\bar{K}}^* \frac{\partial M_{\bar{K}}^*}{\partial M_n^*} - V_{\bar{K}} \frac{\partial V_{\bar{K}}}{\partial M_n^*} \right) \\
 & + m_\sigma^2 \langle \sigma \rangle \frac{\partial \langle \sigma \rangle}{\partial m_n^*} + m_\delta^2 \langle \delta_3 \rangle \frac{\partial \langle \delta_3 \rangle}{\partial m_n^*} + m_{\sigma^*}^2 \langle \sigma^* \rangle \frac{\partial \langle \sigma^* \rangle}{\partial m_n^*} \\
 & - m_\omega^2 \langle \omega_0 \rangle \frac{\partial \langle \omega_0 \rangle}{\partial m_n^*} - m_\rho^2 \langle \rho_{03} \rangle \frac{\partial \langle \rho_{03} \rangle}{\partial m_n^*} - m_\phi^2 \langle \phi_0 \rangle \frac{\partial \langle \phi_0 \rangle}{\partial m_n^*} = 0,
 \end{aligned} \tag{15}$$

$$\begin{aligned}
 & \sum_Y \frac{\partial m_Y^*}{\partial m_\Lambda^*} M_Y \rho_{SY} + M_\Lambda \sum_{Y \neq \Lambda} \frac{\partial V_{0Y}}{\partial M_\Lambda^*} \rho_Y + M_\Lambda \sum_{\bar{K}} (f \theta_{\bar{K}})^2 \left(M_{\bar{K}}^* \frac{\partial M_{\bar{K}}^*}{\partial M_\Lambda^*} - V_{\bar{K}} \frac{\partial V_{\bar{K}}}{\partial M_\Lambda^*} \right) \\
 & + m_{\sigma^*}^2 \langle \sigma^* \rangle \frac{\partial \langle \sigma^* \rangle}{\partial m_\Lambda^*} - m_\phi^2 \langle \phi_0 \rangle \frac{\partial \langle \phi_0 \rangle}{\partial m_\Lambda^*} = 0,
 \end{aligned} \tag{16}$$

where

$$C_{VN} = g_{pp\omega}^* g_{nn\rho}^* + g_{nm\omega}^* g_{pp\rho}^*, \tag{17}$$

$$C_{V\Lambda} = g_{\Lambda\Lambda\omega}^* / g_{\Lambda\Lambda\phi}^*. \tag{18}$$

We omit the explicit expressions of the derivatives in the above equations because their derivations are tedious but straightforward tasks.

Below the K^- threshold $\mu_{K^-} < M_{K^-}^* + V_{K^-}$, Eqs. (11)-(16) with $\theta_{\bar{K}} = 0$ are solved together with the baryon number conservation

$$\rho_T = \sum_{\substack{B=p,n,\Lambda,\Sigma^+, \\ \Sigma^0,\Sigma^-, \Xi^0,\Xi^+}} \rho_B, \tag{19}$$

and the charge neutral condition

$$\sum_{i=B,l,K^-} q_i \rho_i = 0, \tag{20}$$

by means of 8-rank Newton-Raphson method so that we have the three independent effective masses m_p^* , m_n^* and m_Λ^* , and vector potentials, V_p , V_n and V_Λ , and the two independent chemical potentials μ_n and μ_p (or μ_{e^-}). Above the K^- threshold but below the \bar{K}^0 threshold $\mu_{\bar{K}^0} < M_{\bar{K}^0}^* + V_{\bar{K}^0}$, Eqs. (11)-(16) with $\theta_{\bar{K}} = 0$ and Eqs. (19) and (20) are solved together with

$$\mu_{K^-} = M_{K^-}^* + V_{K^-}, \tag{21}$$

by means of 9-rank Newton-Raphson method so that we have the effective masses, the vector potentials, the chemical potentials and the K^- condensation amplitude $f \theta_{K^-}$. Above the \bar{K}^0 threshold, Eqs. (11)-(16) and (19)-(21) are solved together with

$$\mu_{\bar{K}^0} = M_{\bar{K}^0}^* + V_{\bar{K}^0}, \tag{22}$$

by means of 10-rank Newton-Raphson method so that we have the effective masses, the vector potentials, the chemical potentials, and the K^- and \bar{K}^0 condensation amplitudes.

3 Numerical analyses

In the present paper we use the same meson-baryon coupling constants as the EZM-P in Ref. [16]. In addition, we have to specify the meson-kaon coupling constants. First, the

vector meson coupling constants are determined from the SU(3) symmetry [31]:

$$2g_{KK\omega} = 2g_{KK\rho} = \sqrt{2}g_{KK\phi} = g_{\pi\pi\rho} = 6.04. \quad (23)$$

Then, the σ -meson coupling constant is determined [30] so as to produce a given antikaon optical potential in a saturated nuclear matter:

$$U_{\bar{K}}(\rho_{NM}) = -g_{KK\sigma} \langle \sigma \rangle_{NM} - g_{KK\omega} \langle \omega_0 \rangle_{NM}. \quad (24)$$

The other scalar meson coupling constants are determined through the similar relation to Eq. (23):

$$2g_{KK\sigma} = 2g_{KK\delta} = \sqrt{2}g_{KK\sigma^*}. \quad (25)$$

The value of $U_{\bar{K}}(\rho_{NM})$ is a significant open problem in nuclear physics. The coupled-channel Lippmann-Schwinger calculations [32-34] based on the effective chiral model yield relatively deep potentials $-120\text{MeV} < U_{\bar{K}}(\rho_{NM}) < -100\text{MeV}$. The more refined self-consistent calculations [35,36], in which the K^- optical potential is incorporated in the in-medium K^- propagator, generate much shallower potentials $-66\text{MeV} < U_{\bar{K}}(\rho_{NM}) < -55\text{MeV}$. On the other hand, the phenomenological density-dependent potential fitted to K^- atomic data [37] is very deep, $U_{\bar{K}}(\rho_{NM}) \simeq -170\text{MeV}$. In this respect, it is notable that there are recently reported [38,39] the experimental signals of deeply bound kaonic states in stopped K^- reactions on light nuclei.

We show in Fig. 1 the EOSs of cold β -equilibrated NS matter for three kaon potentials $U_{\bar{K}}(\rho_{NM}) = -120\text{MeV}$, -140MeV and -170MeV . In addition we reproduce the EOS containing only nucleons as hadrons [14] by the dotted-dashed curve. The pressure is calculated by means of the Gibbs-Duhem relation $P = \mu_n \rho_T - \mathcal{E}_F - \mathcal{E}_K$. There are upper limits of the total baryon densities, $\rho_T = 1.480\text{fm}^{-3}$, 1.380fm^{-3} and 1.384fm^{-3} for $U_{\bar{K}}(\rho_{NM}) = -120\text{MeV}$, -140MeV and -170MeV , above which an effective mass of neutron becomes negative. We have stopped our calculations at the densities, but the central baryon densities of the most massive NSs are lower than them as will be shown in Table 1.

As being expected, it is seen that the strange particles soften the EOS. However, in contrast to the preceding works [23-26] the deeper kaon potential produces the stiffer EOS. To understand the physical reason, the particle fractions of NS matter are investigated in Figs. 2-4. There are no Σ s in NS matter because we have chosen [16] a repulsive potential of Σ in a saturated nuclear matter. The threshold of Λ is at $\rho_T = 0.360\text{fm}^{-3}$ irrespective of the kaon potential, above which there appear differences between the dotted-dashed and the other curves in Fig. 1. The threshold of K^- is at $\rho_T = 0.972\text{fm}^{-3}$, 0.521fm^{-3} and 0.365fm^{-3} for $U_{\bar{K}}(\rho_{NM}) = -120\text{MeV}$, -140MeV and -170MeV , respectively. The threshold of \bar{K}^0 is at $\rho_T = 1.220\text{fm}^{-3}$, 1.003fm^{-3} and 0.956fm^{-3} , respectively. The difference between the dashed and dotted curves in Fig. 1 appears just above the threshold

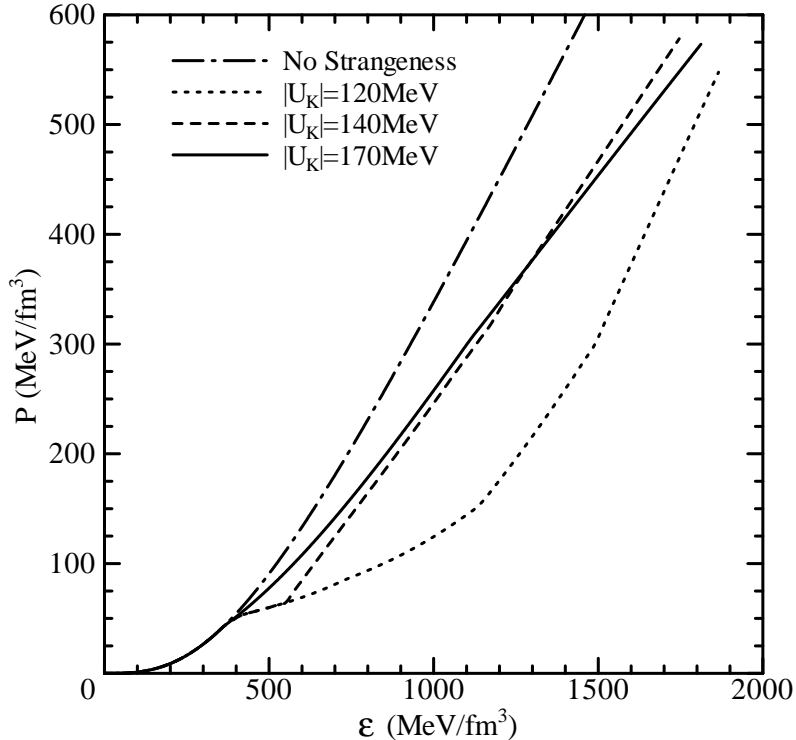


Figure 1: The dotted, dashed and solid curves are the EOSs of cold β -equilibrated NS matter including hyperons and kaons with $U_{\bar{K}}(\rho_{NM}) = -120\text{MeV}$, -140MeV and -170MeV , respectively. The dotted-dashed curve is the EOS including only nucleons as hadrons.

of K^- . On the other hand, the difference between the solid and dotted curve and the difference between the solid and dotted-dashed curve appear at almost the same time, because for $U_{\bar{K}}(\rho_{NM}) = -170\text{MeV}$ the thresholds of Λ and K^- are at almost the same densities.

It is seen in Figs. 2-4 that the deeper kaon potential leads to the earlier appearances of antikaons and tends to exclude the hyperons in NS matter. After the appearances of antikaons, the fractions of Ξ s turn to decrease. This is seen clearly in Fig. 3, where Ξ^- appears at $\rho_T = 0.406\text{fm}^{-3}$ but disappears above $\rho_T = 0.846\text{fm}^{-3}$ while Ξ^0 appears at $\rho_T = 0.916\text{fm}^{-3}$ but disappears above $\rho_T = 1.052\text{fm}^{-3}$. Especially, Ξ s are absent in Fig. 4. The results can be interpreted in a general term. It is energetically favorable that the condensed bosons in the lowest energy state carry strangeness and charge in place of baryons. Because Ξ s have the largest strangeness $|S| = 2$, their abundance indicate strong σ^* mean-field. The stronger $|\langle\sigma^*\rangle|$ leads to a softer EOS. Inversely, less Ξ leads to a stiffer EOS. In another aspect, less Ξ leads to more neutron because of the baryon number conservation and so a larger neutron chemical potential. The EOS therefore becomes stiffer through the Gibbs-Duhem relation. Consequently, the replacement of Ξ s with $S = -2$ by antikaons with $S = -1$ leads to a stiff EOS.

In the preceding works [23-26], for a deep kaon potential the antikaon condensation is the first-order phase transition and so there occurs a mixed phase between the pure

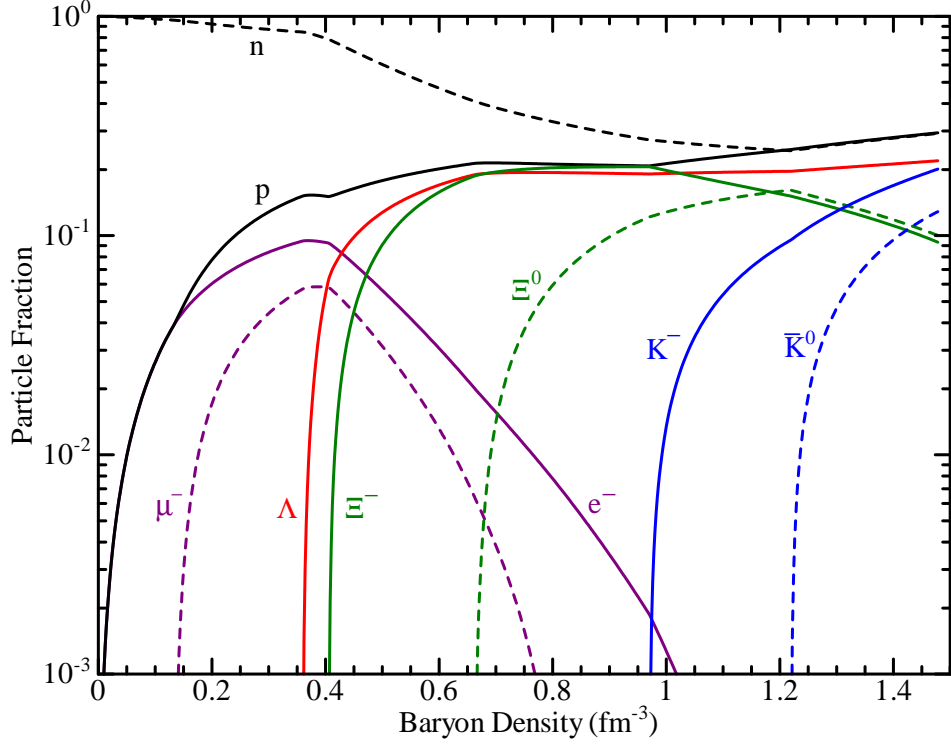


Figure 2: The particle fractions of neutral β -equilibrated NS matter as functions of the total baryon density for $U_{\bar{K}}(\rho_{NM}) = -120\text{MeV}$.

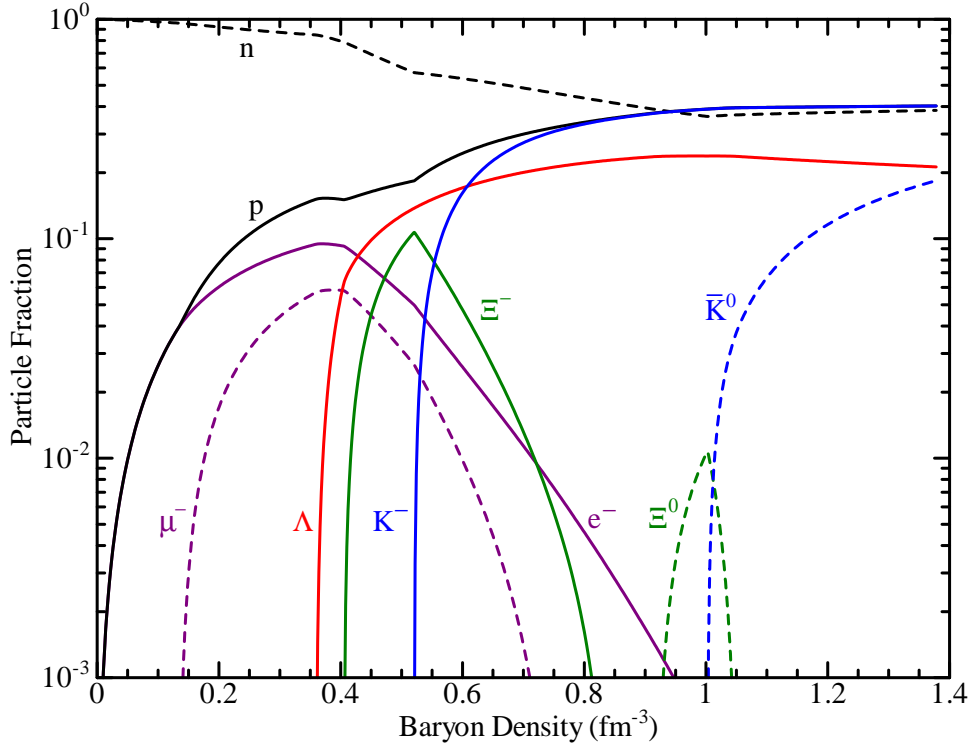


Figure 3: The particle fractions of neutral β -equilibrated NS matter as functions of the total baryon density for $U_{\bar{K}}(\rho_{NM}) = -140\text{MeV}$.

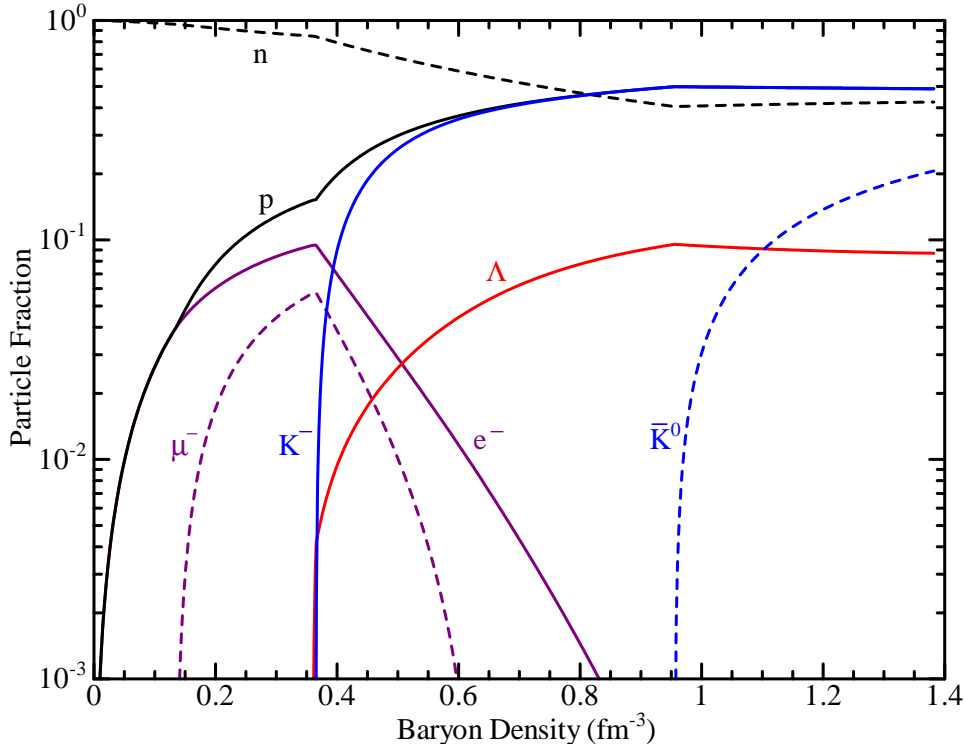


Figure 4: The particle fractions of neutral β -equilibrated NS matter as functions of the total baryon density for $U_{\bar{K}}(\rho_{NM}) = -170\text{MeV}$.

baryon and the antikaon condensed phases. The physically precise construction of the mixed phase is however a serious problem. As has been pointed out in Ref. [30], using the Maxwell construction the electro-chemical potentials in both the phases are not equal. Although Ref. [30] proposes the Gibbs construction, the local charge neutrality is broken. The precise description of the locally charged phase is beyond the RMF theory, in which Coulomb potential is not taken into account. To the contrary, in the EOSs of Fig. 1 the antikaon condensation is the second-order phase transition. This is an attractive feature of the present model because we are not worried about the problem of mixed phase.

In Figure 5 we calculate the mass sequences of non-rotating NSs by integrating the Tolman-Oppenheimer-Volkov (TOV) equation [40]. The EOSs from the EZM models are for the high-density core region of NS. For the outer region below $\rho_T = 0.1\text{fm}^{-3}$ we employ the EOSs by Feynman-Metropolis-Teller, Baym-Pethick-Sutherland and Negele-Vautherin in Ref. [41]. Figure 6 shows the gravitational masses as functions of the central baryon densities. The properties of the most massive NSs with no strange hadrons and for $U_{\bar{K}}(\rho_{NM}) = -120\text{MeV}$, -140MeV and -170MeV are summarized in Table 1. For $U_{\bar{K}}(\rho_{NM}) = -120\text{MeV}$ there is no antikaon in NSs because the central density is lower than the K^- threshold. The result of NS for $U_{\bar{K}}(\rho_{NM}) = -120\text{MeV}$ is therefore the same as the EZM-P in Ref. [16]. However, if the dotted curve in Fig. 5 is investigated carefully, we can find a branch of the third family of compact stars above $\rho_T = 1.327\text{fm}^{-3}$. It is

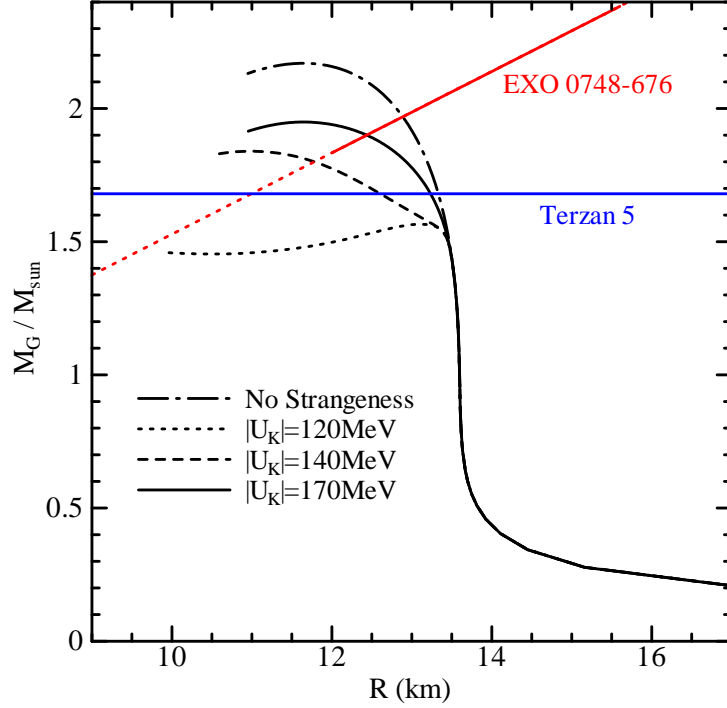


Figure 5: The gravitational mass versus radius of non-rotating NS. The curves are the same as Fig. 1. The blue horizontal line indicates the lower limit of NS mass in Terzan 5 [6]. The red line shows the mass-radius relation of EXO 0748-676 from the redshift [43]. Its solid part is due to Ref. [9].

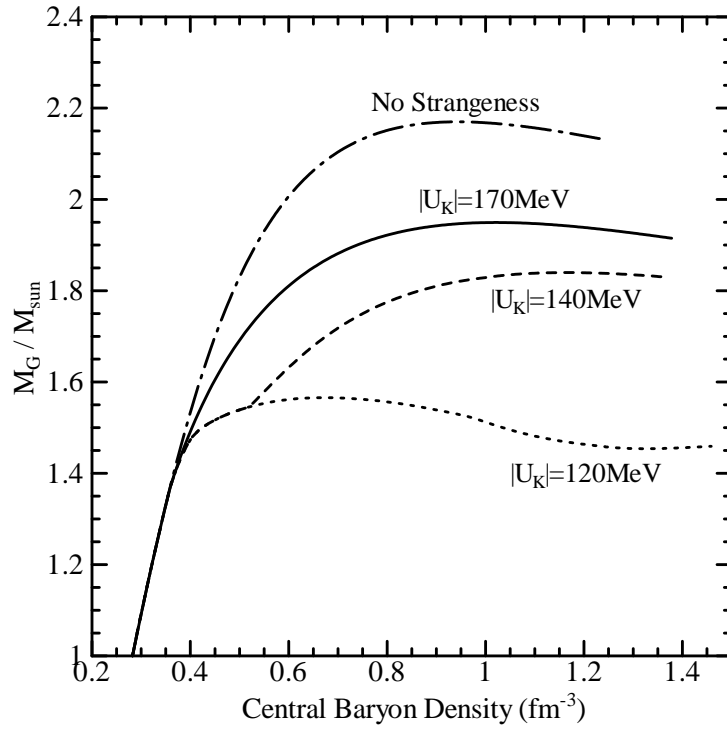


Figure 6: The NS masses as functions of the central baryon densities. The curves are the same as Fig. 1.

Table 1: The properties of the most massive NSs in Fig. 5, the gravitational mass M_G , the radius R and the central baryon density ρ_C , for no strange hadrons [14] and for the antikaon potential $U_{\bar{K}}(\rho_{NM}) = -120\text{MeV}$, -140MeV , -170MeV and -200MeV , respectively.

	$M_G (M_\odot)$	R (km)	ρ_C (fm^{-3})
No strange hadrons	2.17	11.64	0.943
$U_{\bar{K}}(\rho_{NM}) = -120\text{MeV}$	1.57	13.11	0.670
$U_{\bar{K}}(\rho_{NM}) = -140\text{MeV}$	1.84	10.98	1.165
$U_{\bar{K}}(\rho_{NM}) = -170\text{MeV}$	1.95	11.64	1.021
$U_{\bar{K}}(\rho_{NM}) = -200\text{MeV}$	1.87	11.54	1.035

shown by the red solid curve in Fig. 7. The stars on the branch contain the antikaons in their core region. The third family of compact stars due to antikaon condensation was also found in Ref. [42]. Nevertheless, such stars are unlikely to exist in universe, because the dotted curve in Fig. 5 cannot reproduce the recently discovered NS [6] whose gravitational mass is larger than $M_G = 1.68M_\odot$ (shown by the blue horizontal line) in 95% confidence. Only the deeper kaon potentials than $U_{\bar{K}}(\rho_{NM}) = -120\text{MeV}$, for which we find no third family of compact stars, can reproduce it together with another massive NS [8] whose mass is larger than $M_G = 1.6M_\odot$ in 95% confidence and the other more massive NSs [3,4]. Although the other candidates whose masses are heavier than $M_G = 2.0M_\odot$ are reported [2,5], they are not confirmed to be NSs. In the present EZM model with strangeness they must be the low-mass black holes.

Another significant constraint on the EOS of NS matter is obtained from the recently observed redshift [43] of EXO 0748-676, whose mass-radius relation is shown by the red line in Fig. 5. Although the dotted curve cannot satisfy the constraint, the other results are satisfactory. Consequently, if we take into account strangeness in NS matter, most of NSs except for low-mass ones should contain antikaon condensed phase. Moreover, we can find a constraint on the kaon potential from the recent work [9] by Özel, who has succeeded to derive a constraint on mass and radius of EXO 0748-676 shown by the red solid line in Fig. 5. It is seen that only the deeper kaon potential than $U_{\bar{K}}(\rho_{NM}) = -140\text{MeV}$ is allowed. The result is consistent with the recently reported [38,39] experimental signals of deeply bound kaonic states.

For completeness we have also calculated an EOS and NSs using $U_{\bar{K}}(\rho_{NM}) = -200\text{MeV}$ although the results are not shown in figures. Only the property of the most massive NS is listed in Table 1. Because the threshold of Λ is at $\rho_T = 1.20\text{fm}^{-3}$, there are no hyperons in NSs. The absence of hyperons raises the nucleon concentration owing to the baryon number conservation and so the kaon concentration due to the charge neutrality. Therefore, the net fraction of strange contents in NS matter is larger and so the σ^* mean-field

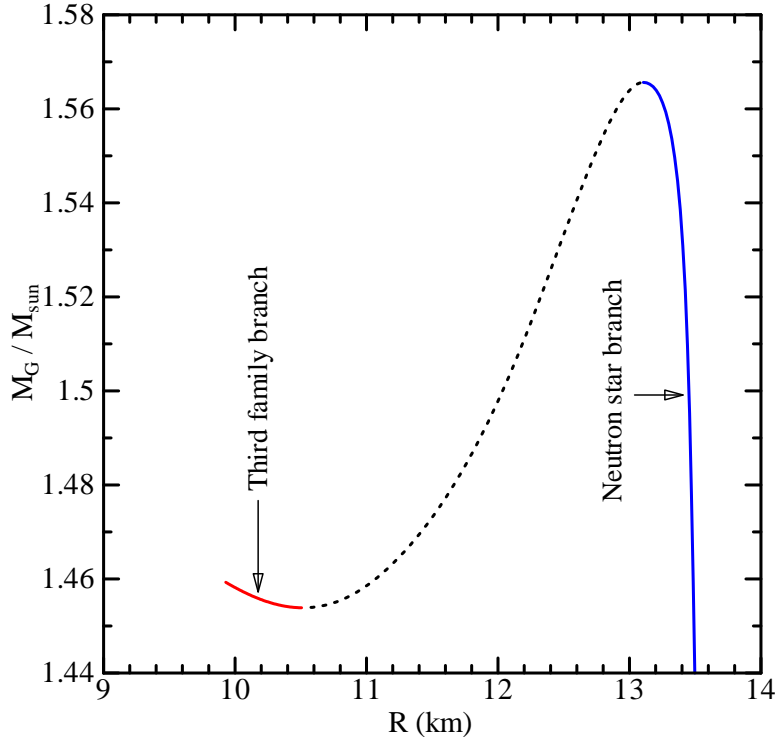


Figure 7: A partial enlargement of the dotted curve in Fig. 5. The blue and red solid curves correspond to the branches of neutron stars and the third family of compact stars.

is stronger than those for $U_{\bar{K}}(\rho_{NM}) = -170\text{MeV}$. Consequently, the EOS becomes softer than the solid curve in Fig. 1. The mass-radius constraint on EXO 0748-676 of the red solid line in Fig. 5 is still satisfied.

Next, we compare our result with the quark-meson coupling (QMC) model in Ref. [25] because it has the field-dependent meson-baryon coupling constants as the EZM model [16] does so. In contrast to our result, there appears K^- in NS even for relatively deep kaon potential $U_{\bar{K}}(\rho_{NM}) \simeq -120\text{MeV}$, and the EOS is softened although the NS mass sequence is similar to the solid curve in Fig. 5. Moreover, all the four results in Fig. 6 of Ref. [25] reproduce the massive NSs and the mass and radius of EXO 0748-676. We are however obliged to present a few questions on the paper. First, for the low-mass NSs of $M_G < M_\odot$ the mass-radius relation with nucleons and hyperons does not agree with that with only nucleons. This is odd because there are no hyperons in the low-mass NSs. In fact, the corresponding results in Ref. [20], which also uses QMC model but does not consider antikaon condensation, agree with each other in $M_G < 1.2M_\odot$. Second, even if the calculation with only nucleons is correct, it predicts a larger radius of NS with $M_G = 1.4M_\odot$ than the upper limit $R = 14.4\text{km}$ [44] estimated recently from J1748+2446ad. Third, the meson-hyperon coupling constants in Ref. [25] are not consistent to the recent data of hypernuclei so that there are Σ s but no Ξ s in NS matter. Moreover, the isovector-scalar meson and the strange mesons are not taken into account. As seen above, the latter plays a crucial role in our result. We believe that our model is

physically more reasonable than the QMC model in Ref. [25].

Finally, we have to mention our previous work [27], which derived a completely different conclusion from the present work that the antikaon condensation is unlikely in NSs. The previous work used the different formulation of antikaon condensation, the different calculus of β -equilibrated state, the different meson-baryon coupling constants and the renormalized field-dependent meson-kaon coupling constants. However, the essential difference is the last point. For completeness we have recalculated the EOSs in Fig. 1 using the same renormalized kaon coupling constants as Eqs. (9) and (10) in Ref. [27]. The results are similar to those in Ref. [27] although they are not shown in figures. There are no antikaons in NSs even for $U_{\bar{K}}(\rho_{NM}) = -140\text{MeV}$, while for $U_{\bar{K}}(\rho_{NM}) = -170\text{MeV}$ the antikaon condensation generates the first-order phase transition and the resultant EOS is softer than the dotted curve in Fig. 1. This is because the renormalized coupling constants of kaons with the strange mesons in dense NS matter are much weaker than the free ones. Owing to the self-consistent determination of scalar mean-fields, the σ^* mean-field becomes much stronger than that for the solid curve in Fig. 1 so as to compensate the weak renormalized σ^* - K coupling constant. On the other hand, the weak renormalized ϕ - K coupling constant directly leads to much weaker ϕ mean-field than that for the dotted curve in Fig. 1. Consequently, the EOS becomes very soft. In the present work we have interpreted the result in an opposite view to Ref. [27] that the renormalized meson-kaon coupling constants are not physically reasonable. We have therefore used the free meson-kaon coupling constants even in dense NS matter.

4 Summary and conclusion

We have shown in Refs. [14] and [16] that the extended Zimanyi-Moszkowski model is able to reproduce almost the existing NS observations if only nucleons are considered as baryons, while it fails to predict the massive NSs of $M_G > 1.6M_\odot$ and the observation of EXO 0748-676 if the hyperons are taken into account. We have therefore extended the investigation of Ref. [16] so as to include the antikaon condensation in NS matter. Being different from our previous work [27], we have assumed the unrenormalized free meson-kaon coupling constants in dense hadronic matter.

The EOSs of NS matter are investigated for three kaon potentials $U_{\bar{K}}(\rho_{NM}) = -120\text{MeV}$, -140MeV and -170MeV in a saturated nuclear matter, which determine σ - K coupling constant. In contrast to all the preceding works, we find that a deeper kaon potential produces a stiffer EOS. This is because the abundance of antikaons tends to exclude Ξ s in NS matter and so the strange scalar mean-field becomes weaker. For $U_{\bar{K}}(\rho_{NM}) = -120\text{MeV}$ there are no antikaons in NSs, and the massive NSs are not reproduced although we have found a branch for the third family of compact stars. The result using the deeper potential $U_{\bar{K}}(\rho_{NM}) = -140\text{MeV}$ reproduces the massive NSs, but the mass-radius constraint on EXO 0748-676 by Özel is not satisfied. Both

the observations are reproduced by only the result using the very deep kaon potential $U_{\bar{K}}(\rho_{NM}) = -170\text{MeV}$. This is consistent to the recent analysis of K^- atomic data and the recently discovered signals of deeply bound kaonic states. Although there remains a problem on the density-dependence of kaon potential at high densities, we can conclude that the antikaon condensed phase is likely to exist in NSs.

Appendix: Table of EOSs

Here, we tabulate the EOSs, the pressure P vs. the baryon density ρ_T and the energy density $\mathcal{E} = \mathcal{E}_F + \mathcal{E}_K$, in the core region $0.08\text{fm}^{-3} \leq \rho_T \leq 1.20\text{fm}^{-3}$ of NS for the kaon potential $U_{\bar{K}}(\rho_{NM}) = -140\text{MeV}$ and -170MeV . Below the threshold of Λ , the two EOSs are equal. For the crust we have used the EOSs in Ref. [41].

$\rho_T(\text{cm}^{-3})$	$U_{\bar{K}}(\rho_{NM}) = -140\text{MeV}$		$U_{\bar{K}}(\rho_{NM}) = -170\text{MeV}$	
	$\mathcal{E}(\text{g} \cdot \text{cm}^{-3})$	$P(\text{dyn} \cdot \text{cm}^{-2})$	$\mathcal{E}(\text{g} \cdot \text{cm}^{-3})$	$P(\text{dyn} \cdot \text{cm}^{-2})$
8.00E+37	1.347325E+14	7.471048E+32	1.347325E+14	7.471048E+32
1.00E+38	1.687169E+14	1.542228E+33	1.687169E+14	1.542228E+33
1.20E+38	2.029225E+14	2.763049E+33	2.029225E+14	2.763049E+33
1.40E+38	2.373981E+14	4.468760E+33	2.373981E+14	4.468760E+33
1.60E+38	2.721813E+14	6.653920E+33	2.721813E+14	6.653920E+33
1.80E+38	3.073065E+14	9.410092E+33	3.073065E+14	9.410092E+33
2.00E+38	3.428106E+14	1.280365E+34	3.428106E+14	1.280365E+34
2.20E+38	3.787297E+14	1.689086E+34	3.787297E+14	1.689086E+34
2.40E+38	4.150990E+14	2.172127E+34	4.150990E+14	2.172127E+34
2.60E+38	4.519518E+14	2.733817E+34	4.519518E+14	2.733817E+34
2.80E+38	4.893200E+14	3.377866E+34	4.893200E+14	3.377866E+34
3.00E+38	5.272335E+14	4.107359E+34	5.272335E+14	4.107359E+34
3.20E+38	5.657202E+14	4.924762E+34	5.657202E+14	4.924762E+34
3.40E+38	6.048062E+14	5.831936E+34	6.048062E+14	5.831936E+34
3.60E+38	6.445155E+14	6.826471E+34	6.445155E+14	6.826471E+34
3.80E+38	6.848203E+14	7.607459E+34	6.847234E+14	7.660124E+34
4.00E+38	7.256889E+14	8.272574E+34	7.251859E+14	8.519081E+34
4.20E+38	7.671369E+14	8.699069E+34	7.659061E+14	9.421564E+34
4.40E+38	8.089685E+14	9.008271E+34	8.068937E+14	1.036845E+35
4.60E+38	8.511292E+14	9.312604E+34	8.481576E+14	1.136011E+35
4.80E+38	8.936116E+14	9.624756E+34	8.897062E+14	1.239655E+35
5.00E+38	9.364142E+14	9.951342E+34	9.315465E+14	1.347759E+35
5.20E+38	9.795375E+14	1.029701E+35	9.736852E+14	1.460284E+35
5.40E+38	1.021219E+15	1.179007E+35	1.016128E+15	1.577180E+35
5.60E+38	1.063301E+15	1.333596E+35	1.058881E+15	1.698386E+35
5.80E+38	1.105846E+15	1.488728E+35	1.101949E+15	1.823829E+35
6.00E+38	1.148836E+15	1.644265E+35	1.145337E+15	1.953431E+35
6.20E+38	1.192252E+15	1.800267E+35	1.189048E+15	2.087107E+35

continued

6.40E+38	1.236070E+15	1.956919E+35	1.233077E+15	2.224748E+35
6.60E+38	1.280274E+15	2.114475E+35	1.277436E+15	2.366286E+35
6.80E+38	1.324850E+15	2.273217E+35	1.322160E+15	2.511688E+35
7.00E+38	1.369788E+15	2.433425E+35	1.367255E+15	2.660859E+35
7.20E+38	1.415082E+15	2.595353E+35	1.412725E+15	2.813709E+35
7.40E+38	1.460728E+15	2.759206E+35	1.458576E+15	2.970148E+35
7.60E+38	1.506720E+15	2.925058E+35	1.504813E+15	3.130089E+35
7.80E+38	1.553063E+15	3.093165E+35	1.551440E+15	3.293449E+35
8.00E+38	1.599775E+15	3.263927E+35	1.598460E+15	3.460147E+35
8.20E+38	1.646857E+15	3.437271E+35	1.645878E+15	3.630106E+35
8.40E+38	1.694302E+15	3.612931E+35	1.693695E+15	3.803251E+35
8.60E+38	1.742088E+15	3.790103E+35	1.741915E+15	3.979511E+35
8.80E+38	1.790263E+15	3.970614E+35	1.790539E+15	4.158815E+35
9.00E+38	1.838839E+15	4.154849E+35	1.839570E+15	4.341096E+35
9.20E+38	1.887808E+15	4.341888E+35	1.889006E+15	4.526291E+35
9.40E+38	1.937023E+15	4.523626E+35	1.938851E+15	4.714334E+35
9.60E+38	1.986547E+15	4.705257E+35	1.989848E+15	4.903542E+35
9.80E+38	2.036401E+15	4.888497E+35	2.043964E+15	5.089457E+35
1.00E+39	2.086594E+15	5.073980E+35	2.098607E+15	5.277609E+35
1.02E+39	2.140060E+15	5.309274E+35	2.153771E+15	5.467932E+35
1.04E+39	2.194303E+15	5.545026E+35	2.209453E+15	5.660361E+35
1.06E+39	2.248423E+15	5.766863E+35	2.265648E+15	5.854828E+35
1.08E+39	2.302697E+15	5.984057E+35	2.322352E+15	6.051265E+35
1.10E+39	2.357455E+15	6.203843E+35	2.379559E+15	6.249603E+35
1.12E+39	2.412695E+15	6.426153E+35	2.437266E+15	6.449773E+35
1.14E+39	2.468415E+15	6.650917E+35	2.495466E+15	6.651703E+35
1.16E+39	2.524614E+15	6.878066E+35	2.554154E+15	6.855321E+35
1.18E+39	2.581290E+15	7.107528E+35	2.613325E+15	7.060555E+35
1.20E+39	2.638439E+15	7.339230E+35	2.672972E+15	7.267329E+35

References

- [1] J.M. Lattimer, "Neutron Stars as a Probe of the Equation of State" in 22nd Texas Symposium on Relativistic Astrophysics at Stanford University (2004).
- [2] J.S. Clark *et al.*, *Astron. Astrophys.* **392** (2002) 909.
- [3] C.O. Heinke, J.E. Grindlay, D.A. Lloyd and P.D. Edmonds, *Astrophys. J.* **588** (2003) 452.
- [4] H. Quaintrell *et al.*, *Astron. Astrophys.* **401** (2003) 313 [arXiv:astro-ph/0301243].
- [5] T. Shahbaz *et al.*, *Astrophys. J.* **616** (2004) L123 [arXiv:astro-ph/0409752].
- [6] S.M. Ransom *et al.*, *Science* **307** (2005) 892 [arXiv:astro-ph/0501230].

- [7] D. Barret, J-F. Olive, M.C. Miller, Mon. Not. Roy. Astron. Soc. **361** (2005) 855 [arXiv:astro-ph/0505402].
- [8] D.J. Nice *et al.*, arXiv:astro-ph/0508050.
- [9] F. Özel, arXiv:astro-ph/0605106.
- [10] T.M. Braje and R.W. Romani, Astrophys. J. **580** (2002) 1043.
- [11] J.E. Trümper, V. Burwitz, F. Haberl and V.E. Zavlin, arXiv:astro-ph/0312600.
- [12] G.B. Rybicki, C.O. Heinke, R. Narayan and J.E. Grindlay, arXiv:astro-ph/0506563.
- [13] T. Klähn, *et al.*, arXiv:nucl-th/0602038.
- [14] K. Miyazaki, Mathematical Physics Preprint Archive (mp_arc) 06-103.
- [15] F. Hofmann, C.M. Keil and H. Lenske, Phys. Rev. C **64** (2001) 025804 [arXiv:nucl-th/0008038].
- [16] K. Miyazaki, Mathematical Physics Preprint Archive (mp_arc) 06-175. (We mistyped the first terms in Eqs. (47) and (48) so that the nucleon mass M_N was missed.)
- [17] M. Baldo, G.F. Burgio and H.-J. Schulze, Phys. Rev. V **61** (2000) 055801 [arXiv:nucl-th/9912066].
- [18] I. Vidana, A. Polls and A. Ramos, Phys. Rev. C **62** (2000) 035801 [arXiv:nucl-th/0004031].
- [19] N.K. Glendenning and S.A. Moszkowski, Phys. Rev. Lett. **67** (1991) 2414.
- [20] S. Pal, M. Hanauske, I. Zakout, H. Stöcker and W. Greiner, Phys. Rev. C **60** (1999) 015802 [arXiv:nucl-th/9905010].
- [21] I. Bednarek, M. Keska and R. Manka, Phys. Rev. C **68** (2003) 035805, [arXiv:nucl-th/0212065].
- [22] B.D. Lackey, M. Nayyar and B.J. Owen, Phys. Rev. D **73** (2006) 024021 [arXiv:astro-ph/0507312].
- [23] R. Knorren, M. Prakash and P.J. Ellis, Phys. Rev. C **52** (1995) 3470 [arXiv:nucl-th/9506016].
- [24] S. Banik and D. Bandyopadhyay, Phys. Rev. C **66** (2002) 065801 [arXiv:astro-ph/0205532].
- [25] D.P. Menezes, P.K. Panda and C. Providência, Phys. Rev. C **72** (2005) 035802 [arXiv:astro-ph/0506196].

- [26] K. Miyazaki, Mathematical Physics Preprint Archive (mp_arc) 05-206
- [27] K. Miyazaki, Mathematical Physics Preprint Archive (mp_arc) 05-233.
- [28] J.M. Weisberg and J.H. Taylor, Proceedings of August 2002 meeting “Radio Pulsars” in Chania, Crete, ASP Conference Series Vol. CS-302 (2003), M. Bailes, D.J. Nice and S.E. Thorsett, eds. [arXiv:astro-ph/0211217].
- [29] J.A. Pons, S. Reddy, P.J. Ellis, M. Prakash and J.M. Lattimer, Phys. Rev. C **62** (2000) 035803 [arXiv:nucl-th/0003008].
- [30] N.K. Glendenning and J. Schaffner, Phys. Rev. C **60** (1999) 025803 [arXiv:astro-ph/9810290].
- [31] J. Schaffner and I.N. Mishustin, Phys. Rev. C **53** (1996) 1416 [arXiv:nucl-th/9506011].
- [32] V. Koch, Phys. Lett. B **337** (1994) 7.
- [33] T. Waas and W. Weise, Nucl. Phys. A **625** (1997) 287.
- [34] A. Ramos and E. Oset, arXiv:nucl-th/9810014.
- [35] A. Ramos and E. Oset, Nucl. Phys. A **671** (2000) 481.
- [36] A. Cieplý, E. Friedman, A. Gal and J. Mareš, Nucl. Phys. A **696** (2001) 173.
- [37] J. Mareš, E. Friedman and A. Gal, Nucl. Phys. A **770** (2006) 84 [arXiv:nucl-th/0601009].
- [38] T. Suzuki *et al.*, Nucl. Phys. A **754** (2005) 375 [arXiv:nucl-ex/0501013].
- [39] M. Agnello *et al.*, Phys. Rev. Lett. **94** (2005) 212303.
- [40] W.D. Arnett and R.L. Bowers, Astrophys. J. Suppl. **33** (1977) 415.
- [41] V. Canuto, Ann. Rev. Astr. Ap. **12** (1974) 167; **13** (1975) 335.
- [42] S. Banik and D. Bandyopadhyay, Phys. Rev. C **64** (2001) 055805 [arXiv:astro-ph/0106406].
- [43] J. Cottam, F. Paerels and M. Mendez, Nature **420** (2002) 51 [arXiv:astro-ph/0211126].
- [44] J.W.T. Hessels *et al.*, arXiv:astro-ph/0601337.